Supporting Information for

Enhanced Electrochemical Performance of Aqueous Zn-Ion Batteries Based on $Na_2V_6O_{16}\cdot 2H_2O$ Cathodes: Insights from DFT and Synchrotron X-ray Analysis

Younghee So[1,‡], Huncheol Seo [2,‡], Seung Hwan Lee[3,‡], Eunseo Lee[1,4], Jinyoung Lee [1,4], Joonhee Kang[5], Young Yong Kim[6,*], Byung-Hyun Kim [2,7,*], Sungwook Mhin[1,4, *]

[1]Department of Materials Science and Engineering, Kyonggi University, Suwon 16227, Republic of Korea

[2]Department of Applied Chemistry, Center for Bionano Intelligence Education and Research, Hanyang University ERICA, Ansan 15588, Republic of Korea

[3]School of Mechanical Engineering, Hanyang University, 222 Wangsimni-Ro, SeongDong-Gu, Seoul, 04763, Republic of Korea

[4]Department of Energy and Materials Engineering, Dongguk University-Seoul, Seoul 04620, Republic of Korea

[5]Department of Nanoenergy Engineering, Pusan National University, Busan 46241, Republic of Korea

[6]Beamline Division, Pohang Accelerator Laboratory, POSTECH, Pohang 37673, Republic of Korea

[7]Department of Chemical and Molecular Engineering, Hanyang University ERICA, Ansan 15588, Republic of Korea

*Correspondence and request for materials should be addressed to S. Mhin (swmhin@kgu.ac.kr), Y. Y. Kim (kimyy@postech.ac.kr), and B.-H. Kim (bhkim00@hanyang.ac.kr)

KEYWORDS. Aqueous zinc-ion battery, charge/discharge cycle, cathode material, $Na_2V_6O_{16}\cdot 2H_2O$ (NaVO), sonochemical synthesis.

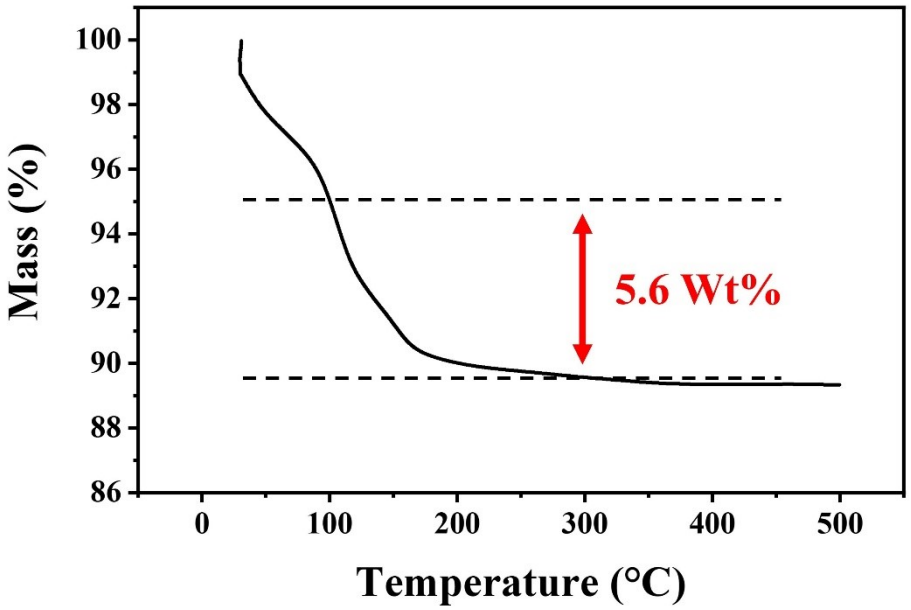

Figure. S1 TGA curve of NaVO

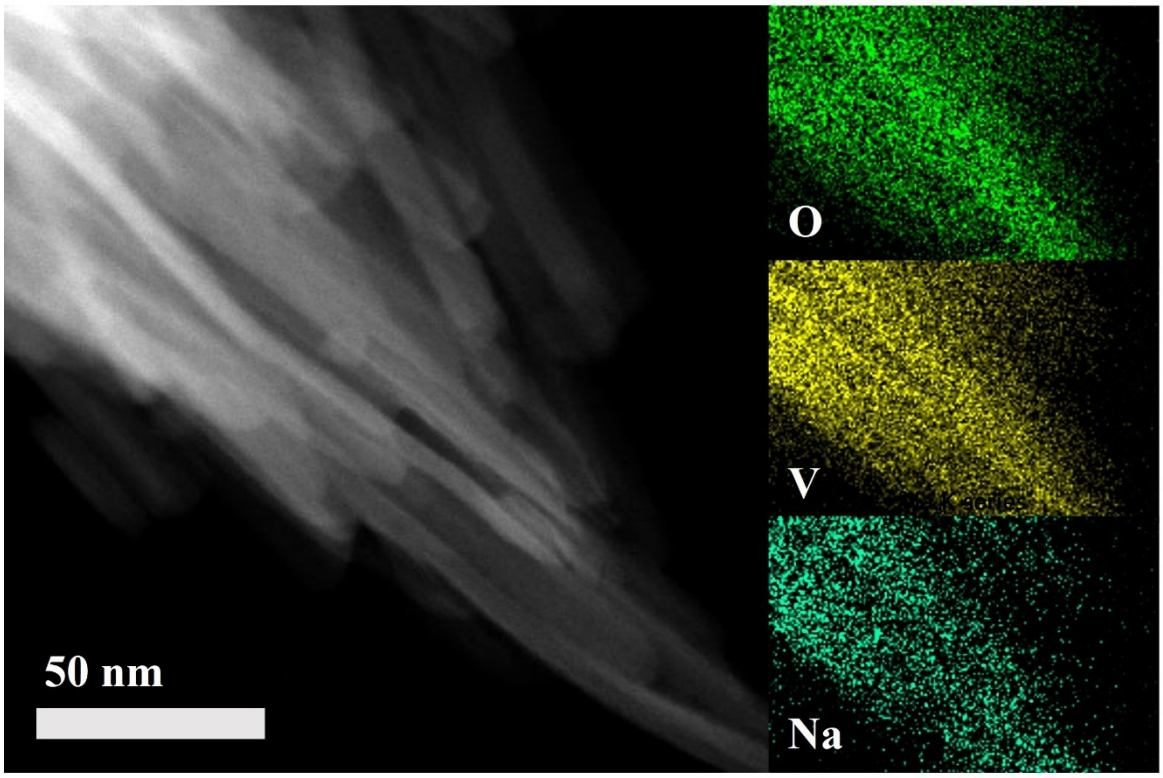

Figure. S2 TEM image and EDX mapping of NaVO

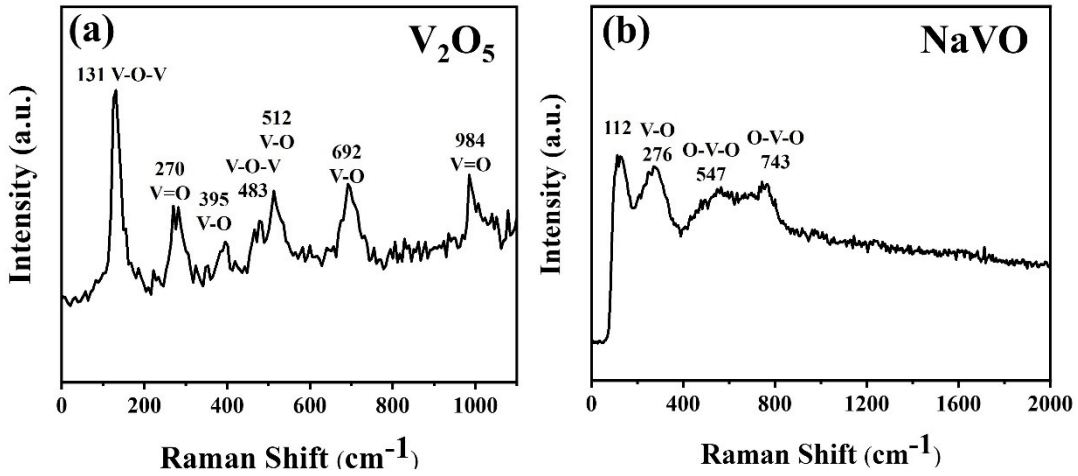

Fig. S3. Raman spectra of (a) V_2O_5 and (b) NaVO

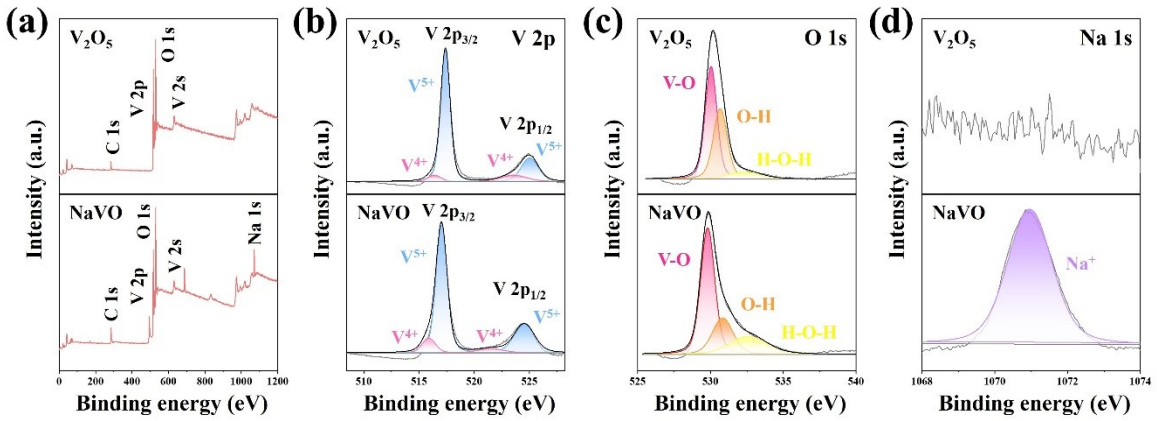

Figure. S4 Characteristics of the V_2O_5 and NaVO from XPS spectra. (a) The wide survey scan of V_2O_5 and NaVO. A narrow scan data and fitted curves of V 2p, O 1s, and Na 1s are shown in (b), (c), and (d), respectively.

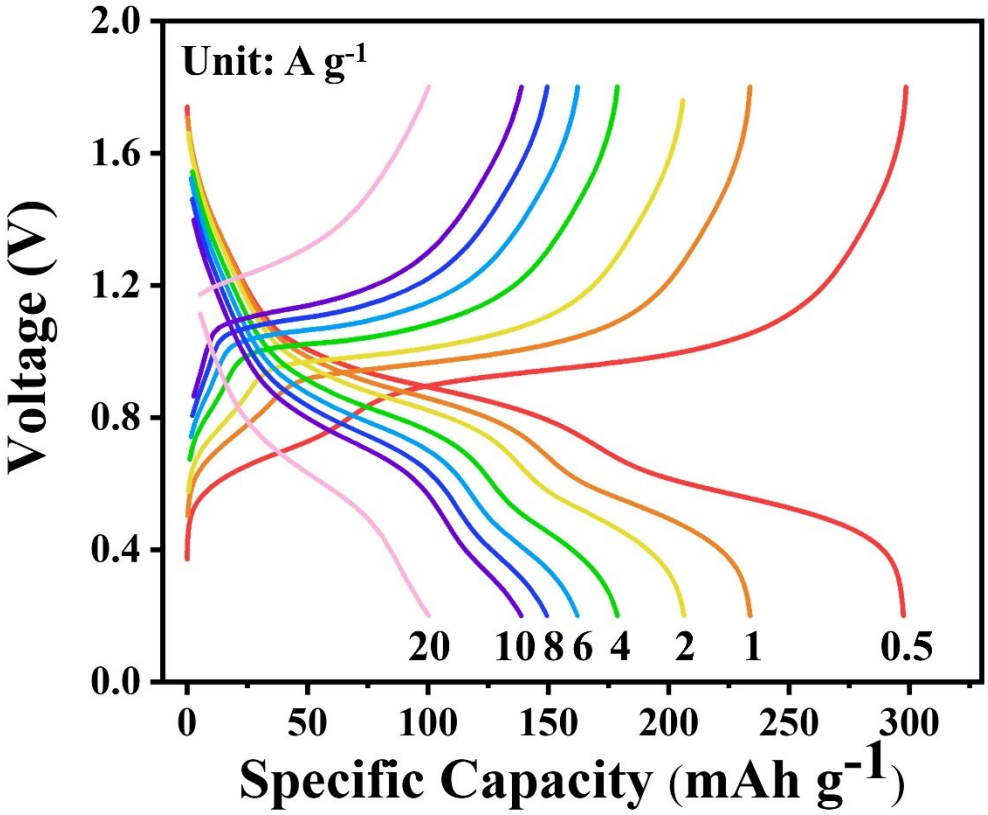

Figure. S5 Chage/Difcharge curve of NaVO//Zn at 0.5, 1, 2, 4, 6, 8, 10 and 20 A g^{-1} respectively.

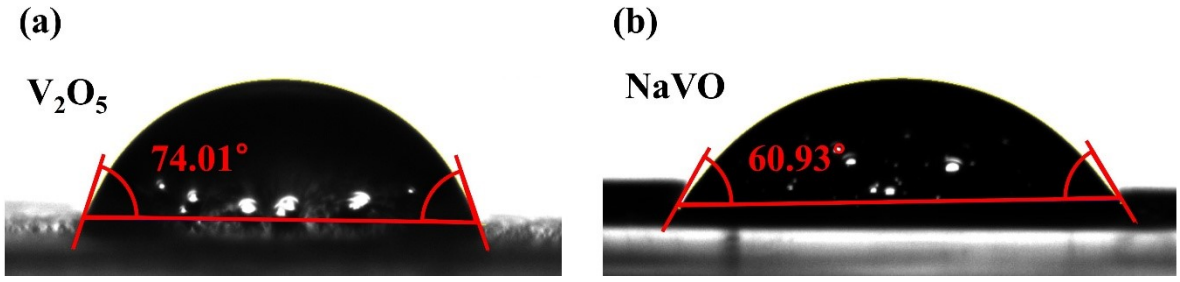

Figure. S6 The contact angles of electrolyte on (a) V_2O_5 and (b) NaVO cathode.

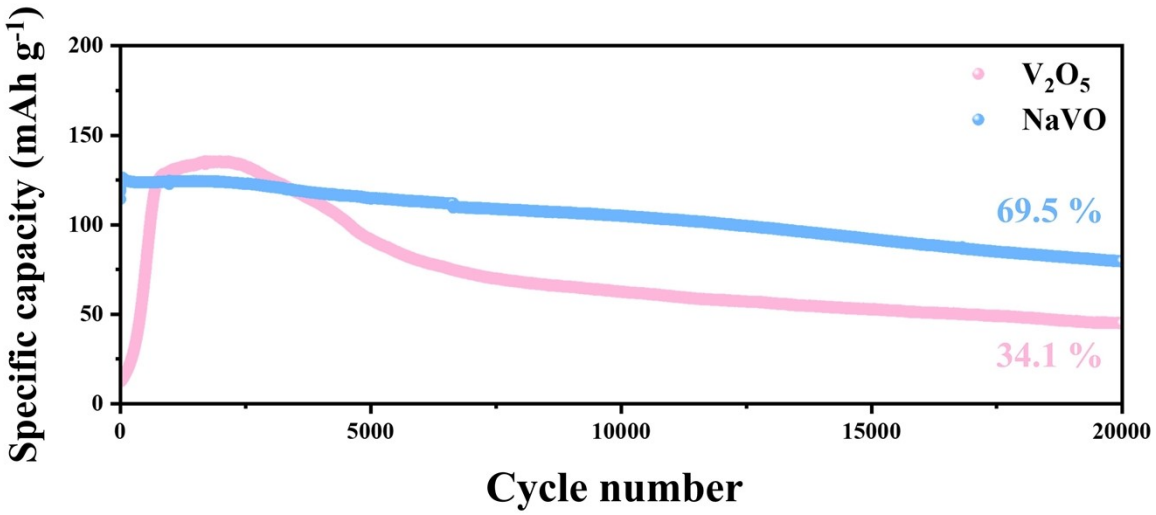

Figure. S7 Cycling performance of NaVO//Zn and V_2O_5//Zn at 10A g^{-1}.

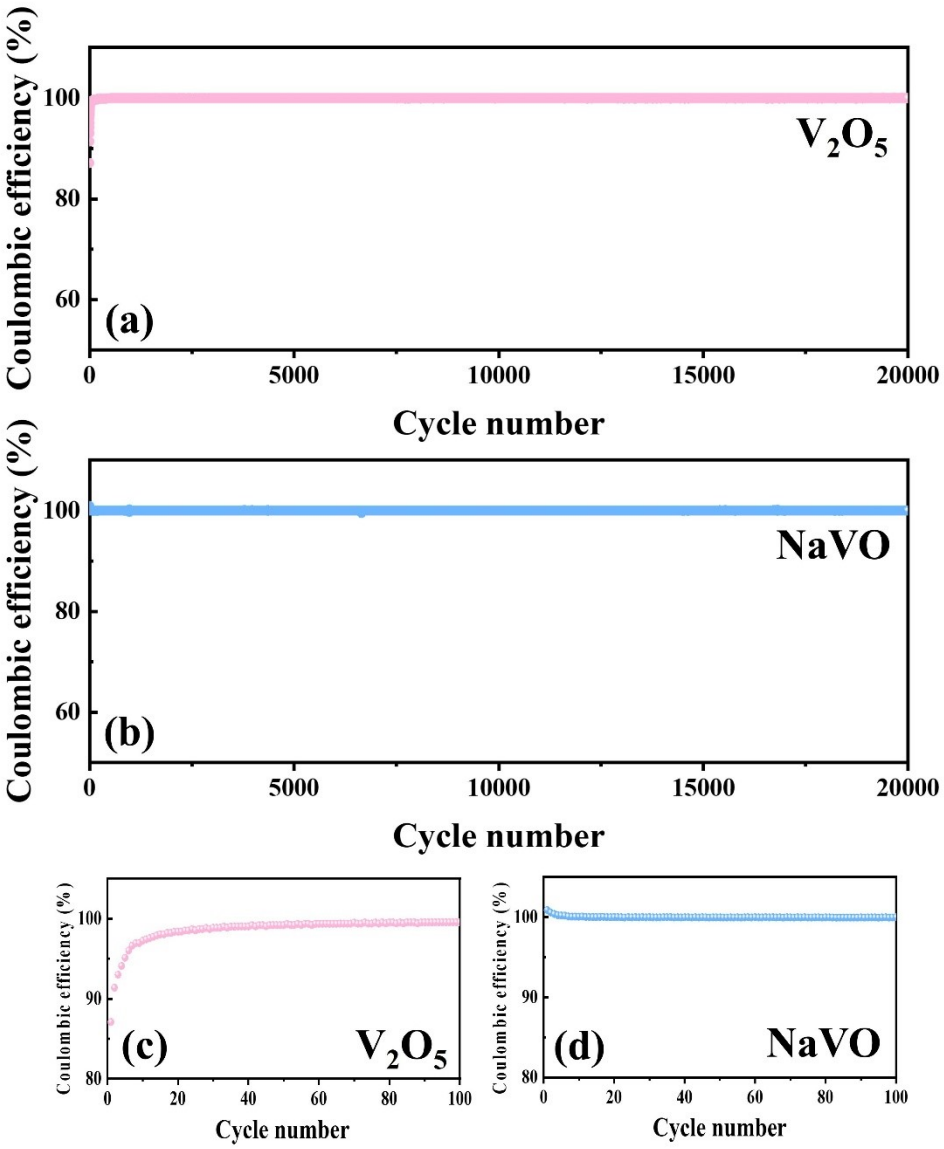

Figure. S8 Coulombic efficiency of (a) NaVO and (b) V_2O_5 for 10000 cycles. Coulombic efficiency of (c) NaVO and (d) V_2O_5 for 100 cycles.

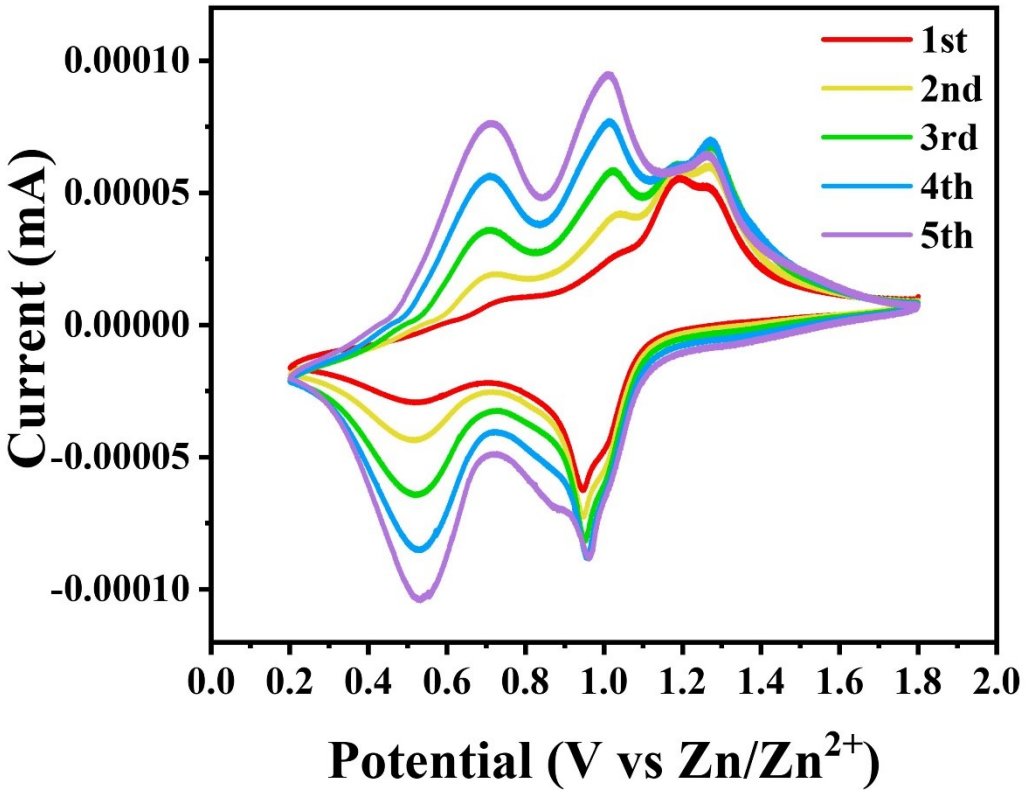

Figure. S9 CV curves of V_2O_5//Zn for 5 cycles at scan rates from 0.1 mV s^{-1}.

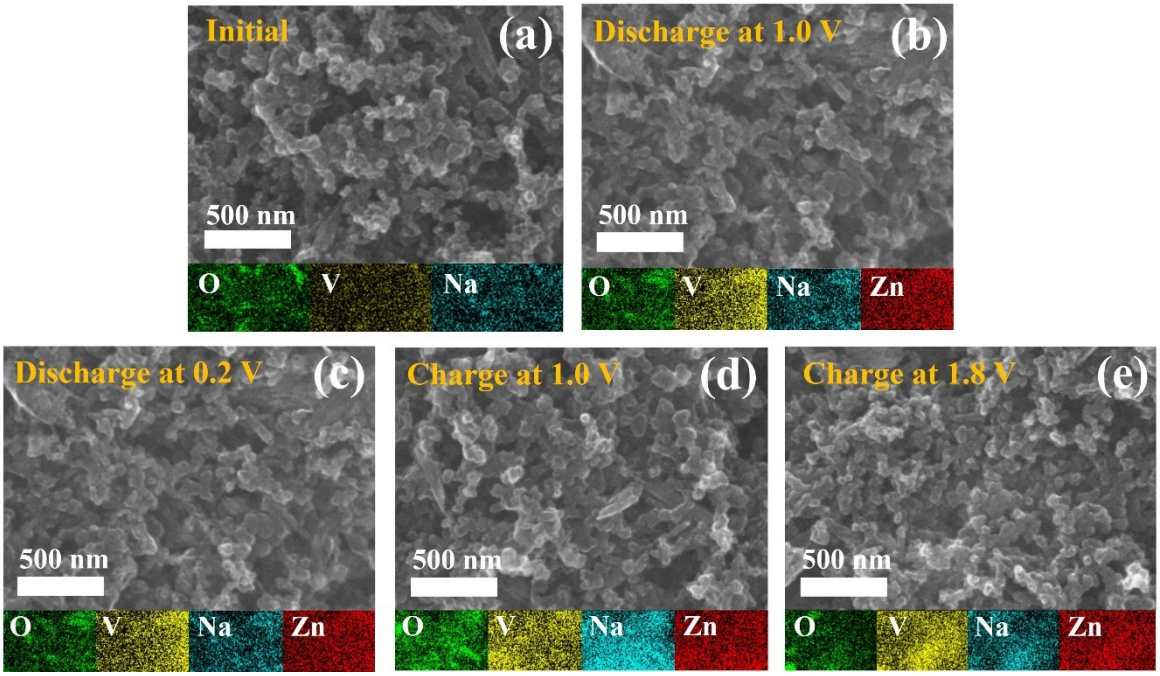

Figure. S10 SEM images and EDS mapping of NaVO (a) Initial (b) Discharge at 1.0 V (c) Discharge at 0.2 V (d) Charge at 1.0 V and (e) Charge at 0.2 V.

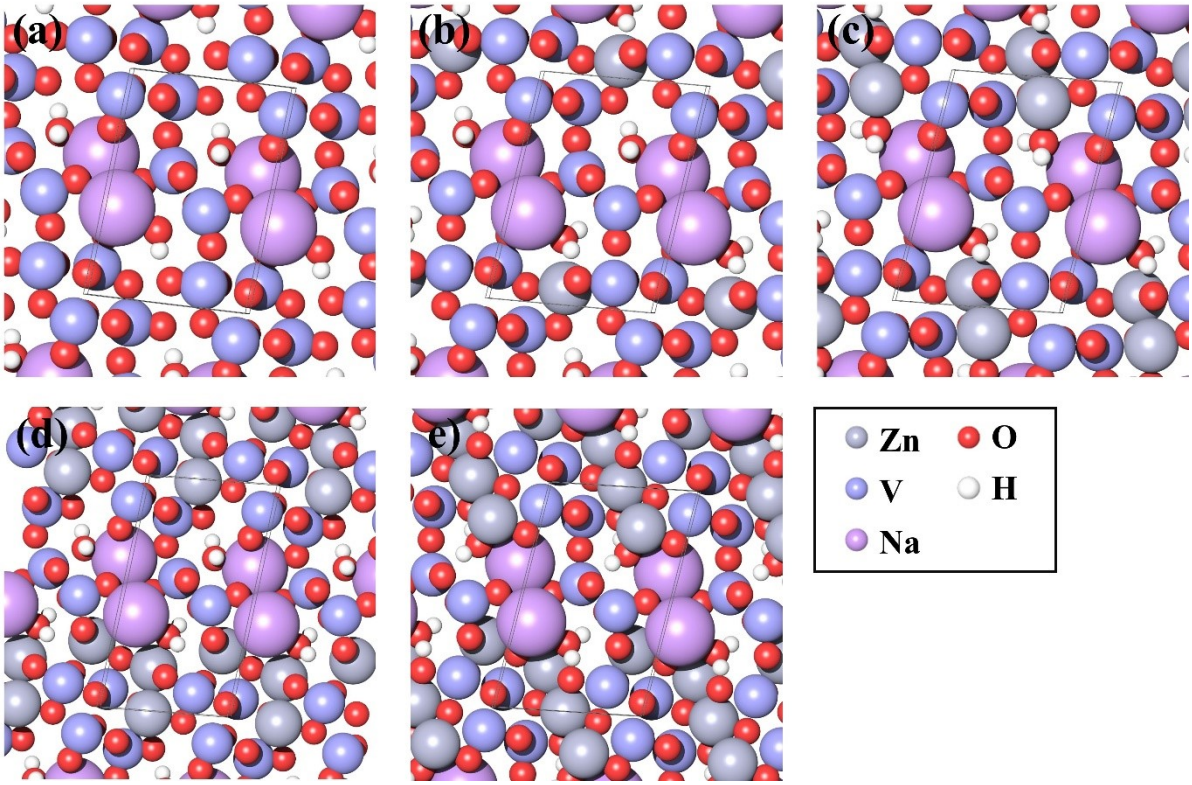

Figure. S11 Optimized structural configurations of NaVO with Zn intercalation at concentrations of (a) 0, (b) 1, (c) 2, (d) 3, and (e) 4 Zn ions. (Zn: gray, V: blue, Na: violet, O: red, H: white)

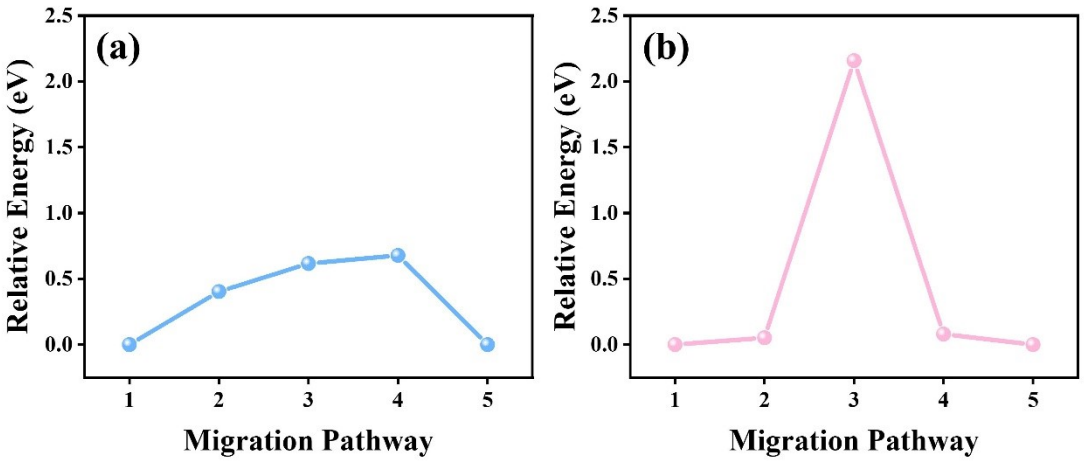

Figure. S12 Relative energy for Zn ion migration between equivalent sites in (a) NaVO and (b) V_2O_5 cathodes along the pathway.

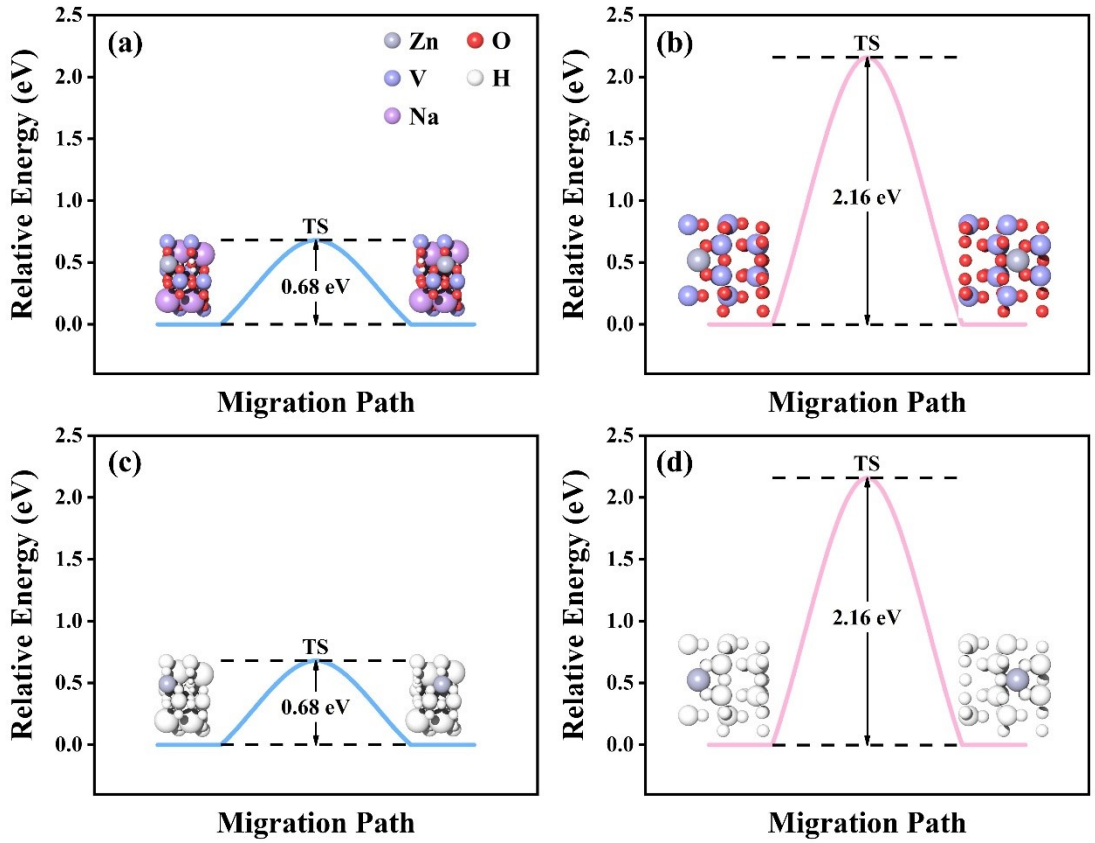

Figure. S13 Relative energy plot of initial, transition and final state during Zn migration between equivalent sites in (a), (c) NaVO and (b), (d) V_2O_5 cathodes. (Zn: gray, V: blue, Na: violet, O: red, H: white)

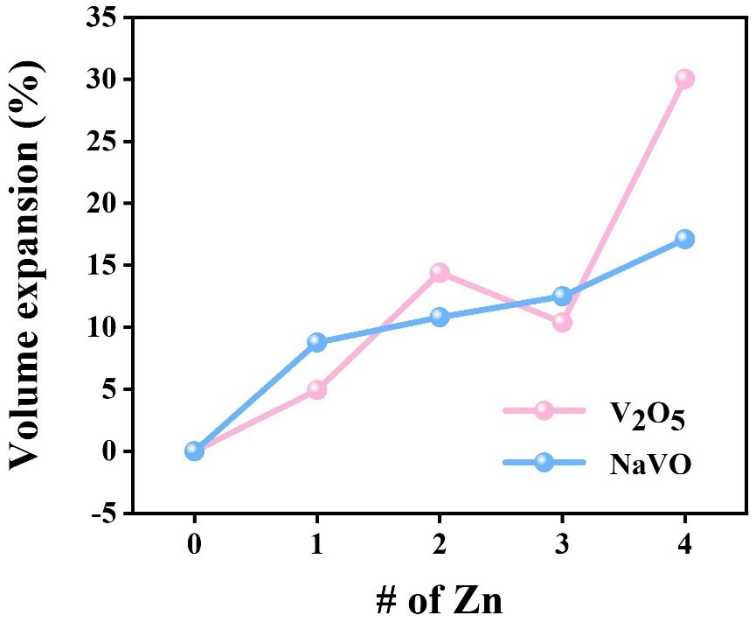

Figure. S14 Comparison of volume expansion ratio in NaVO and V_2O_5 cathodes during Zn intercalation.

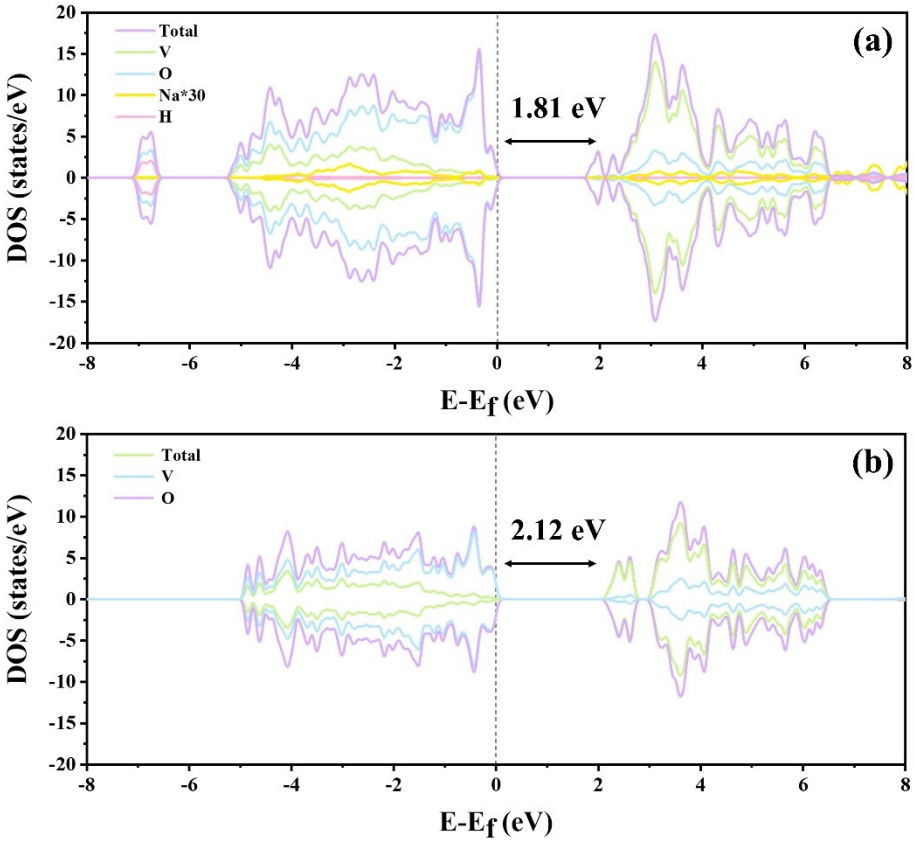

Figure. S15 Electronic density of states for (a) NaVO and (b) V_2O_5

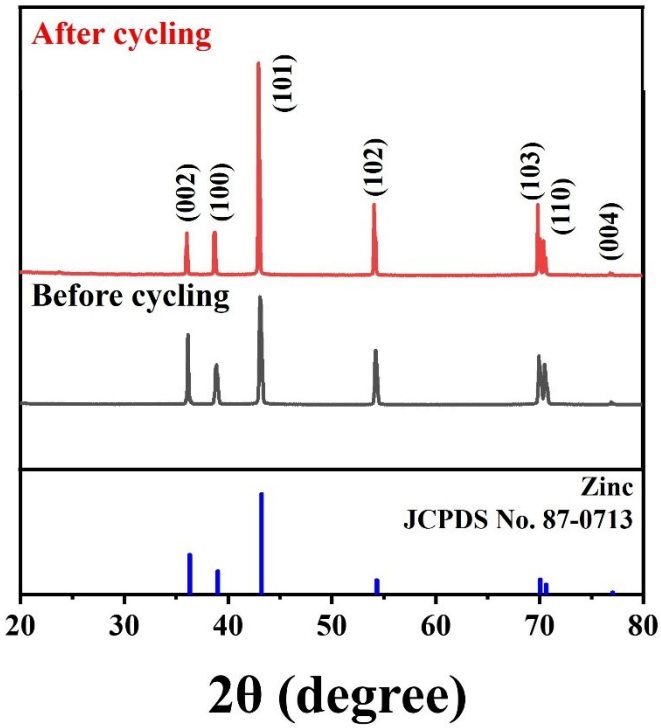

Figure. S16 The XRD patterns of Zinc Anode before and after cycling.

V_2O_5	Charge percentage (%)	Volume (Å^3)	Volume expansion (%)
0 Zn	100	183.005	0
1 Zn	75	192.051	4.94
2 Zn	50	209.354	14.40
3 Zn	25	202.005	10.38
4 Zn	0	237.972	30.04

NaVO	Charge percentage (%)	Volume (Å^3)	Volume expansion (%)
0 Zn	100	331.857	0
1 Zn	75	360.952	8.77
2 Zn	50	367.730	10.81
3 Zn	25	373.357	12.50
4 Zn	0	388.608	17.10

Table S1. Comparison of volume expansion ratio in NaVO and V_2O_5 cathodes during Zn intercalation.

Cathode Material	Electrolyte	Synthetic method	Voltage range (V)	Specific Capacity (mAh g^{-1})	Cycling performance (cycles)	Reference
$Na_2V_6O_{16}·2H_2O$	$Zn(CF_3SO_3)_2$	Sonochemical	0.2-1.8	126.3 at 10 A g^{-1}	10000	This work
$Na_2V_6O_{16}·3H_2O$	$Zn(ClO_4)_2$/PC	hydrothermal	0.2-1.7	142 at 5 A g^{-1}	5000	[1]
$Na_2V_6O_{16}·2.14H_2O$	$ZnSO_4/Na_2SO_4$	hydrothermal	0.2-1.6	116 at 20 A g^{-1}	2000	[2]
$Na_2V_6O_{16}·1.66H_2O$	$ZnSO_4/Na_2SO_4$	hydrothermal	0.2-1.6	102 at 5 A g^{-1}	1800	[3]
$Na_2V_6O_{16}·3H_2O$	$ZnSO_4$	Microwave-Assisted Hydrothermal	0.4-1.4	152 at 15 A g^{-1}	1000	[4]

Table S2. Comparison of this work with previous studies on Zn-ion battery cathodes

[1] Tan, Huiteng, et al., Free-Standing Hydrated Sodium Vanadate Papers for High-Stability Zinc-Ion Batteries. *Batteries & Supercaps* 3.3 (2020): 254-260.

[2] Hu, Fang, et al., $Na_2V_6O_{16}·2.14H_2O$ nanobelts as a stable cathode for aqueous zinc-ion batteries with long-term cycling performance. *Journal of Energy Chemistry* 38 (2019): 185-191.

[3] Qin, Liping, et al., Improved working voltage and high rate performance of sodium vanadate cathode materials for aqueous zinc ion batteries by altering synthetic solution pH guiding the structure change. *Materials Today Communications* 31 (2022): 103460.

[4] Soundharrajan, Vaiyapuri, et al., $Na_2V_6O_{16}·3H_2O$ barnesite nanorod: an open door to display a stable and high energy for aqueous rechargeable Zn-ion batteries as cathodes. *Nano letters* 18.4 (2018): 2402-2410.